Volcanology, geochemistry and structural geology of the Upper Cretaceous Hidalgo Formation, southwestern New Mexico

John R. Young, Nancy J. McMillan, Timothy F. Lawton, and Richard P. Esser
2000, pp. 149-156. https://doi.org/10.56577/FFC-51.149

in:

Southwest Passage: A trip through the Phanerozoic, Lawton, T. F.; McMillan, N. J.; McLemore, V. T.; [eds.], New Mexico Geological Society 51 st Annual Fall Field Conference Guidebook, 282 p. https://doi.org/10.56577/FFC-51

This page is intentionally left blank to maintain order of facing pages.

VOLCANOLOGY, GEOCHEMISTRY AND STRUCTURAL GEOLOGY OF THE UPPER CRETACEOUS HIDALGO FORMATION, SOUTHWESTERN NEW MEXICO

JOHN R. YOUNG[1], NANCY J. McMILLAN[2], TIMOTHY F. LAWTON[2], and RICHARD P. ESSER[3]
[1]New Mexico Environment Department Hazardous and Radioactive Materials Bureau, 2044A Galisteo, Santa Fe, NM 87505; laramide@excite.com; [2]Department of Geological Sciences, Box 3AB, New Mexico State University, Las Cruces, New Mexico 88003; nmcmilla@nmsu.edu; tlawton@nmsu.edu; [3]New Mexico Bureau of Mines and Mineral Resources, New Mexico Institute of Mining and Technology, 801 Leroy Place, Socorro, New Mexico, 87801; esser@nmt.edu.

Abstract—The Hidalgo Formation represents the proximal cone-forming lithofacies association of a dominantly andesitic, Laramide stratovolcano. New $^{40}Ar/^{39}Ar$ age determinations of 70.53 ± 0.48, 70.69 ± 0.44 Ma, and 71.44 ± 0.38 Ma demonstrate an Upper Cretaceous age of volcanism. Early Hidalgo volcanism is recorded by plagioclase-bearing lava flows, lapilli tuff, ash-fall tuff, and debris-flow breccia intercalated with sandstone, shale and conglomerate of the underlying Upper Cretaceous Ringbone Formation. The base of the Hidalgo Formation is marked by an abrupt transition to predominantly autoclastic, monolithologic and heterolithologic breccia, and cogenetic massive lava flows with subordinate intrusions and sedimentary deposits. Laramide shortening accompanied volcanism and resulted in the folding of the Hidalgo Formation into an overturned footwall syncline adjacent to the Hidalgo thrust fault. Whole-rock analyses of 19 lava, intrusion, and cumulate xenolith samples indicate that Hidalgo magmas range from basalt to andesite (48–60% SiO_2, 2.7–7.3% MgO). Hidalgo lavas were variably altered during cooling, diagenesis, and intrusion of the mid-Tertiary Eureka complex; the rocks now contain high and variable volatile contents (1.3–8.5% loss on ignition). Concentrations of the soluble elements K, Na, Rb, Ba, and Sr have been modified and do not reflect the original igneous concentrations; however, insoluble elements such as the rare earth elements, Ta, Ti, Zr, and Hf, appear to have been unaffected by alteration. Fractionation of the observed mineral assemblage plagioclase + hornblende + augite in lavas, dikes, and cumulate xenoliths is consistent with major element trends and a slight depletion of the middle rare-earth elements in evolved lavas. Low Ta/La ratios (0.035–0.076) are similar to modern continental arcs and suggest that Hidalgo volcanism was triggered by subduction of the Farallon Plate during Laramide shortening.

INTRODUCTION

The Laramide orogeny, a major mountain-building event in western North America from 80 to 40 Ma, has been ascribed to low-angle subduction of the Farallon plate under the west coast of North America (Snyder et al., 1976; Dickinson and Snyder, 1978). The low-angle subduction model is based on the observation that ages of arc volcanic and plutonic rocks decrease regularly from west to east prior to and during the Late Cretaceous and early Tertiary Laramide orogeny. Dickinson et al. (1976) and Coney and Reynolds (1977) inferred from these data that the decreasing dip of the subducting Farallon plate caused eastward migration of volcanism and Laramide deformation in the southwestern United States, similar to the modern amagmatic segment of the central Andes of Chile and Argentina that overlies a flat-slab segment of the oceanic Nazca plate (Kay and Abbruzzi, 1996). The southern Laramide volcanic arc is generally characterized by peraluminous, mineralized silicic stocks, other plutons, and related silicic volcaniclastic rocks (Lipman and Sawyer, 1985; Keith and Wilt, 1986; Titley and Anthony, 1988).

A deformed but relatively complete sequence of Upper Cretaceous–lower Tertiary (Laramide) synorogenic deposits crops out in the northern Little Hatchet Mountains of extreme southwestern New Mexico (Fig. 1; Lawton et al., 1993). Included within this section is the Hidalgo Formation, a remnant of a Laramide volcanic complex (Lawton et al., 1993) that offers a unique opportunity to study less differentiated magmatic systems associated with Laramide orogenic activity. This paper presents stratigraphic, structural, petrographic geochronologic, and geochemical data, which indicate that the Hidalgo Formation represents a deformed, eroded Laramide composite continental-arc volcano and supports the flat-slab subduction model.

AGE, REGIONAL STRATIGRAPHY, AND STRUCTURAL GEOLOGY

Laramide deformation, deposition, and volcanism are recorded in the Little Hatchet Mountains by a 3200-m-thick section of sedimentary and volcanic rocks (Lawton et al., 1993). The lower part of this consists of 950–1600 m of interbedded conglomerate, sandstones, and mudstone (Hodgson, 1991; Lawton et al., 1993) of the Upper Cretaceous Ringbone Formation. Upper Cretaceous andesitic breccias and lava flows of the Hidalgo Formation were deposited conformably above the Ringbone Formation. The Laramide section is underlain by the Lower Cretaceous Hell-to-Finish, U-Bar, and Mojado formations, which consist of 4200 m of sandstone, shale, and limestone deposits correlative with the Bisbee Group of southeastern Arizona and southwestern New Mexico (Hodgson, 1991; Hodgson this volume). Eocene andesitic volcaniclastic deposits, possibly equivalent to the Eocene Palm Park or Rubio Peak formations, lie with angular unconformity above the Laramide section. The coarse-grained Hatchet Gap granite exposed in the southern Little Hatchet Mountains (Zeller, 1970; Hodgson, 1991) is presumed to be late Proterozoic or early Paleozoic in age (Channell et al., this volume).

The age of the Hidalgo is Late Cretaceous based on new $^{40}Ar/^{39}Ar$ age determinations (Table 1, Fig. 2). Hornblende mineral separates from two samples yield excellent and identical $^{40}Ar/^{39}Ar$ plateau ages of 70.69 ± 0.44 (sample 99PP3) and 70.53 ± 0.48 (sample HDV-127) Ma, which correspond well to an $^{40}Ar/^{39}Ar$ determination of 71.44 ± 0.38 Ma on a hornblende phenocryst from a breccia clast (sample NM-679, Lawton et al., 1993). Sample 99PP3 was taken from the basal heterolithologic breccia clast of the Hidalgo Formation on Howells Ridge; sample HDV-127 was taken from a hornblende bearing basaltic lava flow found approximately 0.5 km northeast of the Hidalgo thrust fault in the northern part of the range.

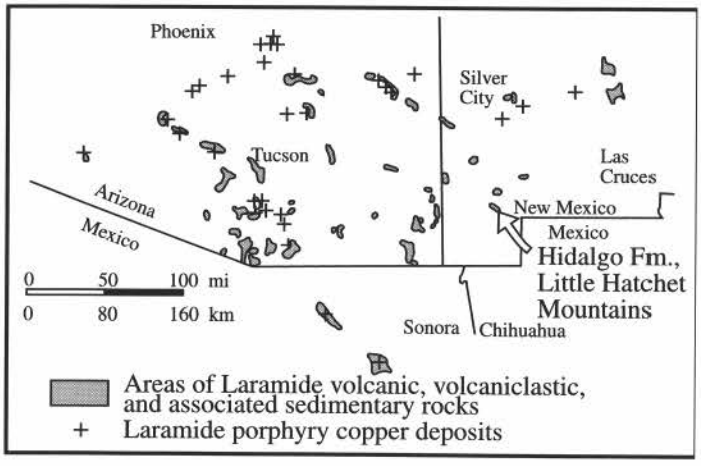

FIGURE 1. Location of Laramide igneous centers in southeast Arizona and southern New Mexico. Modified from Titley and Anthony (1988).

TABLE 1. Isotopic data for $^{40}Ar/^{39}Ar$ age determinations for samples from the Hidalgo Formation.

ID		Temp (°C) or Power (w)	$^{40}Ar/^{39}Ar$	$^{37}Ar/^{39}Ar$	$^{36}Ar/^{39}Ar$ (x 10^{-3})	$^{39}Ar_K$ (x 10^{-16} mol)	K/Ca	$^{40}Ar^*$ (%)	^{39}Ar (%)	Age (Ma)	±1σ (Ma)
NM679 hornblende, wt. = 97.13 mg, J = 0.003507 ± 0.25%, D = 1.004 ± 0.002, RD79, Lab # = 17											
B		1150	9.60	7.74	-5.66	346.0	0.129	117.4	4.1	69.96	0.56
C		1200	11.43	7.31	-0.12	1718	0.137	100.3	20.3	71.11	0.12
D	¥	1250	11.48	7.23	-0.12	34033	0.138	100.3	40.3	71.43	0.14
E	¥	1350	11.41	7.77	-0.36	29722	0.129	100.9	35.2	71.44	0.10
Total gas age				n = 5		84496	0.069			71.4	1.8*
plateau			MSWD +3.7*	n = 2	steps D–E	63372	0.134		75.5	71.44	0.38*
99-PP-3 horblende, wt. = 19.87 mg, J =0.0008184 ± 0.10%, D = 1.00644 ± 0.00091, NM-115, Lab # = 50700-01											
A		800	2146	4.756	712	1.41	0.11	1.9	1.2	59	41
B		850	207.9	15.74	620.7	1.14	0.032	12.4	2.1	38.2	4.2
C		950	100.8	6.894	275.1	0.802	0.074	19.9	2.8	29.6	2.7
D		1020	51.64	2.184	81.14	0.979	0.23	53.9	3.7	40.7	1.3
E		1080	81.78	2.103	162.3	0.882	0.24	41.6	4.4	49.6	2.0
F		1120	49.02	3.468	33.84	1.42	0.15	80.2	5.6	57.30	0.86
G		1160	48.01	5.090	12.55	3.07	0.10	93.2	8.2	65.14	0.47
H	¥	1200	50.40	5.853	8.690	36.2	0.087	95.9	38.8	70.33	0.14
I	¥	1300	49.60	5.876	4.784	68.4	0.087	98.1	96.5	70.83	0.13
J	¥	1400	53.80	6.110	18.61	3.65	0.084	90.7	99.6	71.04	0.44
K		1650	137.6	5.409	318.5	0.465	0.094	31.9	100.0	64.1	4.7
total gas age				n = 11		118.5	0.090			69.2	1.5*
plateau			MSWD = 3.8**	n = 3	steps H–J	108.3	0.087		91.4	70.69	0.44*
HDV-127 hornblende, wt. = 4.65 mg, J = 0.0008187 ± 0.10%, D = 1.00644 ± 0.00091, NM-115, Lab # = 50701-01											
A		5	1171	7.473	3824	0.483	0.068	3.5	1.6	60	49
B		10	402.6	16.32	1256	0.939	0.031	8.2	4.7	48.6	7.9
C		12	70.99	7.165	99.02	1.25	0.071	59.6	8.9	61.84	0.82
D	¥	16	58.51	7.122	36.26	9.46	0.072	82.7	40.2	70.52	0.19
E	¥	20	60.33	7.321	41.89	9.57	0.070	80.5	72.0	70.78	0.19
F	¥	25	61.00	7.441	46.04	5.17	0.069	78.7	89.1	70.02	0.29
G		30	70.37	8.226	88.24	1.47	0.062	63.9	94.0	65.71	0.81
H		40	73.54	7.974	53.30	1.80	0.064	79.5	100.0	84.93	0.62
total gas age				n = 8		30.1	0.068			69.9	2.6*
plateau			MSWD = 2.5	n = 3	steps D–F	24.2	0.070		80.3	70.53	0.48*

Notes:

Isotopic ratios corrected for blank, radioactive decay, and mass discrimination, not corrected for interferring reactions.

Individual analyses show analytical error only; plateau and total gas age errors include error in J and irradiation parameters.

Sample NM679 from USGS, Reston (Lawton et al. 1993); 99-PP-3 and HDV-127 from this study (NMGRL).

Flux monitor (Fish Canyon sanidine) = 27.84 Ma.

D = Mass discrimination (1 a.m.u.)

Correction factors from USGS: $(^{40}Ar/^{39}Ar)K = 0.0057$; $(^{36}Ar/^{37}Ar)Ca = 0.00026$; and $(^{39}Ar/^{37}Ar)Ca = 0.00067$.

Correction factors at NMGRL: $(^{40}Ar/^{39}Ar)K = 0.0002 \pm 0.0003$; $(^{36}Ar/^{37}Ar)Ca = 0.00026 \pm 0.00002$; and $(^{39}Ar/^{37}Ar)Ca = 0.00070 \pm 0.00005$.

Samples 99-PP-3 and NM679 were analyzed using the resistance furnace, while HDV-127 was analyzed using the CO_2 Laser.

Spectrometer sensitivity at NMGRL: 2.3×10^{-16} moles/pA (Furnace) & 1.3×10^{-16} moles/pA (Laser).

Total system blanks at NMGRL averaged 1250, 8, 1.0, 7.5, 7.0 x 10^{-18} moles at masses 40, 39, 38, 37, and 36, respectively.

Plateau (weighted mean) age calculated by weighting each age analysis by the inverse of the variance.

Plateau (weighted mean) error calculated using the method of Taylor (1982).

K/Ca = molar ratio calculated from reactor produced $^{39}Ar_K$ and $^{37}Ar_{Ca}$.

¥ = steps included in Plateau (weighted mean) age.

** MSWD values using method of Mahon (1996) outside of 95% confidence interval.

* 2s error

Zeller (1970) mapped extensive exposures of mafic–intermediate plutonic rocks in the central Little Hatchet Mountains as possible Laramide intrusions. These rocks, host to the Sylvanite mining district, have been difficult to date because of hydrothermal alteration. However, major and trace element similarities between samples from the Hidalgo Formation (this study) and the Sylvanite intrusive complex (Channell et al., this volume) provide additional evidence for their common Laramide origin.

A complex relationship between the Hidalgo Formation and underlying Upper Cretaceous Ringbone, Lower Cretaceous U-Bar, and Lower Cretaceous Mojado formations is indicated by the variable nature of the unconformity above the Lower Cretaceous formations. At its eastern limit, the Hidalgo Formation rests unconformably on the Lower Cretaceous Mojado and U-Bar formations (Zeller, 1970; Hodgson, 1991; Lawton et al., 1993). Over most of its extent, however, the Hidalgo-Ringbone contact is gradational as indicated by the presence of plagioclase-phyric lava flows, ash fall tuff, lapilli tuff, and volcaniclastic breccia intercalated with the conglomerate, sandstone, siltstone, and mudstone of the upper member of the underlying Ringbone Formation (Zeller, 1970; Basabilvazo, 1991; Lawton et al., 1993). A Late Campanian to Maastrichtian age for the upper member of the Ringbone Formation is interpreted from pollen, wood, and dinosaur fossils (Zeller, 1970; Lawton et al., 1993), making the Ringbone Formation similar in age to Hidalgo lavas. These relations indicate that the Ringbone and Hidalgo formations onlap the Lower Cretaceous section as a genetic unit.

During the Laramide orogeny, the region experienced two-stage deformation (Hodgson, 1991). The west–northwest-trending basement-block Hidalgo uplift located to the southwest of the complimentary Ringbone basin initially developed in the early Campanian due to movement along the existing Granite Pass thrust fault (Seager and Mack,

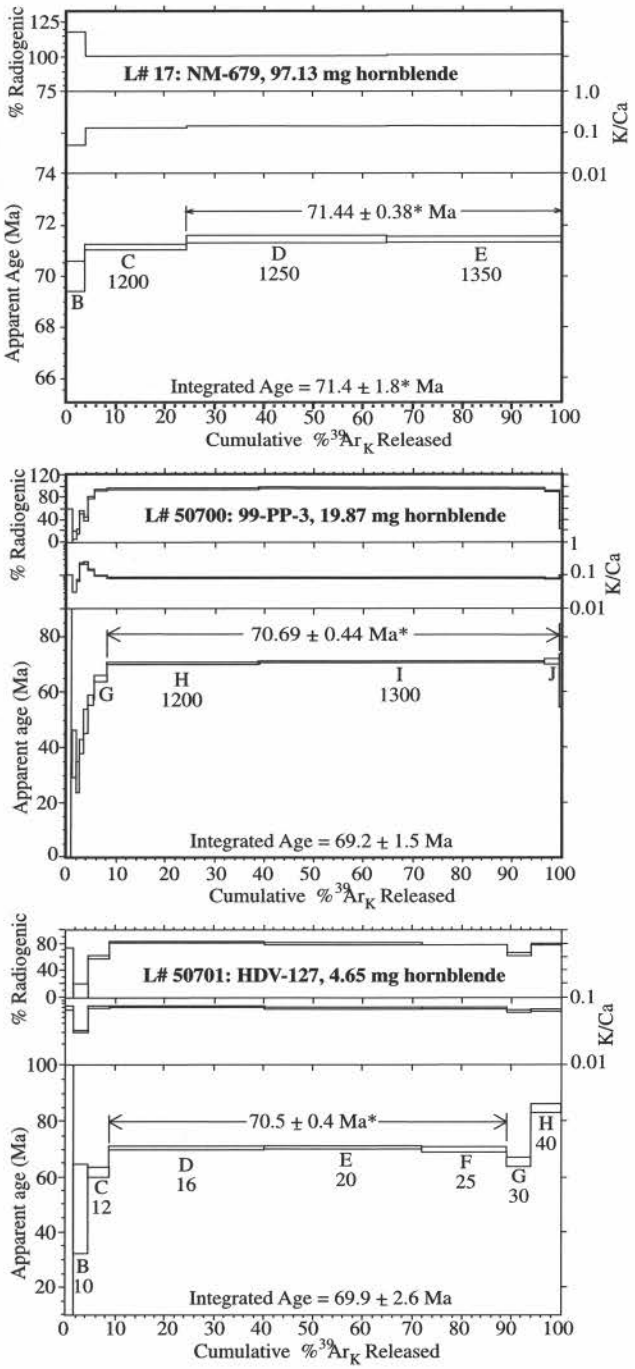

FIGURE 2. $^{40}Ar/^{39}Ar$ spectra for new age determinations of samples from the Hidalgo Formation.

1986; Hodgson, 1991) in the southern the Little Hatchet Mountains. Hodgson (1991) suggests that Paleocene–early Eocene left-lateral wrenching along the Granite Pass fault followed development of block uplift-basin pairs. Northeast-vergent thrust faults developed (e.g., the Mojado and Hidalgo thrust faults) as the result of wrenching and subsequently divided the Ringbone basin into separate depocenters (Hodgson, 1991; Lawton et al., 1993). Hidalgo volcanism began during the first stage of deformation and continued through the development of the Hidalgo and Mojado thrust faults (Hodgson, 1991; Lawton et al., 1993). Continued movement along the Hidalgo thrust folded the Hidalgo Formation into an overturned footwall syncline, the axis of which is subparallel to the trace of the thrust fault. The minimum age of thrusting is constrained by a K/Ar age determination of 58 ± 2.0 Ma on a diorite sill that intrudes the Howells Ridge thrust (Loring and Loring, 1980).

DESCRIPTION AND CLASSIFICATION OF LITHOFACIES

One of the goals of this study is to understand the volcanology of the Hidalgo Formation. In spite of alteration and limited exposure, the original lithologic character of the Hidalgo Formation is well preserved at many localities. The Hidalgo Formation consists of a suite of lithofacies typical of composite cones: complex, laterally discontinuous, interbedded monolithologic breccias, autobreccias, heterolithologic breccias, massive lava flows, dikes, block and ash flows, and reworked volcanic and sedimentary detritus. These facies are described in the following paragraphs.

Monolithologic breccia

Monolithologic breccias are composed dominantly of angular–subrounded, pebble- to boulder-sized clasts of porphyritic plagioclase (± hornblende) basalt to andesite set in a clay- to sand-sized matrix of volcanic grains of the clast lithology. Some clasts exhibit fracture patterns that could reflect either in situ cooling or fragmentation due to clast-to-clast impacts during deposition (Smith et al., 1999). Monolithologic breccias are either clast- or matrix-supported. The amount of matrix is generally inversely proportional to the degree of clast roundness, with the breccias ranging from angular and clast supported to sub-rounded and matrix-supported. Although the extent of most breccia units was difficult to discern, they appear to be laterally discontinuous and massive with little or no internal stratification or grading. Deposits range in thickness from <1 m to 10 m.

Heterolithologic breccia

Matrix-supported heterolithologic breccias are also common in the Hidalgo Formation. Clast diameter varies, from pebble-size to 3 m. Clasts range from angular to rounded. The matrix consists of clay, lithic fragments, and monocrystalline fragments of plagioclase and hornblende. Crude stratification of poorly sorted coarse pebbles interbedded in heterolithologic breccia was observed in some locations. Breccias are laterally discontinuous and less than 10 m thick.

The clast population in the heterolithologic breccias changes systematically upsection. Near the Hidalgo-Ringbone contact, these breccias include a variety of sedimentary clasts including limestone, limestone conglomerates, and siltstone, as well as scoriaceous, aphanitic, and phaneritic igneous clasts. Igneous clasts tend to be sub-angular and smaller than the well-rounded sedimentary clasts; clast-sizes for both populations are relatively small (<40 cm diameter). The abundance of sedimentary clasts diminishes about 20 m above the Hidalgo-Ringbone contact, and the heterolithologic breccias are composed of texturally variable, angular–rounded, scoriaceous, aphanitic, and porphyritic volcanic clasts, as well as phaneritic diorite clasts. Volcanic clasts are identical in texture and mineralogy to Hidalgo lava flows. Although most individual breccia deposits are coarse-grained (boulder-sized), finer-grained (cobble-sized or smaller) breccias are present. One unique breccia bed contains large (>3 m diameter) sub-angular–angular clasts of porphyritic basalt in a matrix that contains altered euhedral biotite crystals. The biotite is a primary magmatic phase; metasomatism would have affected more than one depositional unit. The presence of biotite suggests this unit resulted from the eruption of an evolved, more viscous Hidalgo magma, possibly related to the rhyolite that intrudes the Hidalgo thrust fault.

Lava flows

Massive lava flows and lava-flow cores constitute 15–20% of the exposed outcrops in the Hidalgo Formation and are present but less common in the upper member of the Ringbone Formation. Individual, massive lava flows are difficult to recognize due to poor exposures and because they tend to have thin (<2 m), narrow cores encased by brecciated bottoms and tops. However, some individual flows exceed 5 m in thickness and are laterally continuous for several tens of meters or more.

Ringbone lava flows differ from Hidalgo flows in mineralogy and dimension. Ringbone flows can be traced laterally for several tens of meters and attain maximum thicknesses of 8 m. Plagioclase is the only phenocryst mineral, indicated by white laths as long as 1.5 cm; ferromagnesian phases are absent. Compositionally, the Ringbone flows are basaltic andesites (RB010, Table 2). Flow indicators, such as vesicle alignment and trachytic plagioclase, in Ringbone lavas suggest the source is parallel to strike, to the northwest or southeast. No evidence of brecciated flow tops or bottoms was observed.

In contrast, lavas in the Hidalgo Formation crop out as thin, narrow lava flows or lava flow cores surrounded by brecciated zones. Compositionally, the Hidalgo flows range from basalt to andesite. Texturally, the flows range from aphanitic to porphyritic. Mineralogically, individual flows contain as much as 50% zoned plagioclase, 25% zoned hornblende, 7% Fe-Ti oxide phenocrysts, and may contain augite (replaced by calcite and clay) phenocrysts in a trachytic, felty, or intergranular groundmass. Hornblende crystals are sometimes unusually large, reaching lengths of several centimeters, commonly with a reaction corona of Fe-Ti oxides and pyroxene. Hornblende-plagioclase-augite cumulate xenoliths similar to those found in dikes in the Ringbone and Hidalgo formations are also present in some lava flows. A few Hidalgo lava flows exhibit crude flow-banding and contain contorted or elongate scoria clasts, suggesting that the clasts were hot and plastic during emplacement. The thickness of these discontinuous flows is difficult to discern, but they may attain thicknesses of several tens of meters.

Intrusions

Numerous dikes and plugs, generally concentrated along or near faults and fractures, occur in the Hidalgo and Ringbone formations. The intrusions range in composition from basalt to rhyolite and are mineralogically similar to the lava flows, although alteration to chlorite, calcite, and epidote obscures primary igneous textures in some cases. Textures range from aphyric to porphyritic; dikes contain phenocrysts and glomerocrysts of zoned hornblende (with reaction rims of Fe-Ti oxides and augite), zoned plagioclase, augite, Fe-Ti oxides, and locally contain altered biotite. Dike width is weakly correlative to composition; basaltic dikes are typically several centimeters to 1 m thick, whereas andesitic dikes are commonly more than 3 m thick. Plugs range from several meters to >100 m in diameter. An unusual plagioclase-, quartz- and biotite-bearing rhyolitic plug intrudes the Hidalgo thrust fault.

Hidalgo intrusions contain phaneritic cumulate xenoliths composed predominantly of plagioclase and hornblende with subordinate augite. Some xenoliths are banded with alternating layers of hornblende and plagioclase whereas others are composed almost entirely of hornblende. In addition, some intrusions contain small (<0.5 mm diameter) rounded xenocrysts of plagioclase, hornblende, and quartz. Mafic enclaves were observed in the rhyolitic intrusion found at the Hidalgo thrust fault.

Sedimentary facies

Siltstone, sandstone, and conglomerate comprise less than 5% of the Hidalgo Formation. Clasts are angular to well rounded and moderately to well sorted. Most beds are thin (<10 cm) and appear laterally continuous; however, some exceed 2 m in thickness. In contrast, more massive and lenticular coarse conglomerate deposits with little observed stratification extend laterally only a few meters (Young, 1996).

Most conglomerate beds are composed entirely of volcanic clasts, similar in composition to the surrounding breccia deposits. The lower conglomerate contains well rounded to subangular clasts, including a variety of igneous clasts, monocrystalline hornblende fragments, siltstone, limestone and limestone-clast conglomerate, and fine-grained sandstone, which are similar to the underlying heterolithologic breccia.

Thin 30-cm beds of siltstone and fine-grained sandstone containing volcanic lithic grains and rounded plagioclase grains separate breccia deposits. Slight scouring of the underlying breccia deposit is evident in some locations. Although planar bedding is common, low-angle cross-bedding is also present. An interval of pebbly fine-grained sandstones with thin planar bedding and low-angle cross-beds crops out intermittently for roughly 0.75 km at the top of the Hidalgo section. This interval appears to thin to the northwest.

VOLCANOLOGICAL INTERPRETATION

We interpret the Hidalgo Formation as the flank facies of a composite cone and that its deposition involved a variety of syn-eruption and less important inter-eruption processes. Our model is based on lithofacies interpretation and comparison of deposits identified at modern volcanic centers. The modern volcanic deposits were interpreted using paleomagnetic data, analysis of clasts, and field relationships (e.g., Parsons, 1969; Cole et al., 1986; Hackett and Houghton, 1989; Grubensky et al., 1998; Smith et al., 1999). Because the Hidalgo Formation is dominated by interbedded monolithologic and heterolithologic breccias, we focus our attention on these deposits.

Monolithologic breccia

Hidalgo monolithologic breccia deposits are attributed to various stages of autobrecciation of cooling or cool, active lava flows cascading down steep slopes (Parsons, 1969; Cole et al., 1986; Hackett and Houghton, 1989; Smith and Grubensky, 1993; Smith et al., 1999). The characteristics of the monolithologic breccia are consistent with autobrecciated deposits observed at more-modern volcanic terranes. These characteristics include: variable clast roundness, variable matrix development, and similar clast/fragment textures and mineralogies to surrounding lava flows and/or lava flow cores (Cole et al., 1986; Hackett and Houghton, 1989; Smith et al., 1999).

Matrix development and clast rounding is initiated as lavas cool, creating blocks and other fragments that are subsequently rounded by abrasion as lavas and/or blocks continue to flow. Continued abrasion and granulation increase the amount of matrix material and enhance clast roundness (Parsons, 1969; Cole et al., 1986; Hackett and Houghton, 1989; Smith et al., 1999) and can result in completely brecciated flows or massive lava cores with brecciated borders (Smith et al., 1999). The degree of rounding and the amount of matrix generated in these friction breccias increase with distance from the source (Parsons, 1969; Cole et al., 1986; Hackett and Houghton, 1989; Smith et al., 1999). At Ruapehu volcano in New Zealand, well-developed autobrecciation of lava flows takes place between 4 and 6 km from the source (Cole et al., 1986; Hackett and Houghton, 1989). Channell et al. (this volume) propose that the Sylvanite intrusive complex, 7 km south of exposed Hidalgo volcanic rocks, is the subvolcanic plumbing system for the Hidalgo composite cone; although the distance between the Sylvanite complex and the Hidalgo Formation has changed during Laramide shortening and Basin-and-Range extension, the degree of autobrecciation is consistent with this proposed correlation.

Heterolithologic breccia

Heterolithologic breccia deposits have been attributed to various processes. Hackett and Houghton (1989) suggest that they originate as cool, wet debris flows or hot block and ash flows. Smith et al. (1999) add that heterolithologic breccias at Ruapehu may form by the incorporation of pyroclastic material into an autobrecciating lava flow, resulting in incorporation of ash and scoriaceous fragments with clasts that are mineralogically and texturally distinct from surrounding lava flows. Heterolithologic breccias may also result from the reworking of volcanic-flank material by wet or dry mass flows (Smith et al., 1999).

Most heterolithologic breccias in the Hidalgo probably represent wet debris-flow deposits. The breccias contain no apparent scoriaceous juvenile volcanic clasts, precluding incorporation of pyroclastic material during lava flow autobrecciation. Deposits of poorly sorted, crudely stratified sands, pebbles, and cobbles that resemble hyper-concentrated flood flow deposits (i.e., Smith, 1986) are interbedded with many heterolithologic breccias. Hyper-concentrated flood-flow deposits form during high-discharge, high-sediment events in which both traction and suspension processes occur during down-stream dilution of a channeled debris flow as it laterally transitions to normal stream flow (Smith, 1986). The association of hyper-concentrated flood-flow deposits with

TABLE 2. Whole-rock major and trace element analyses of Hidalgo samples by ICP. Oxides listed in weight percent; elements listed in ppm.

Sample	HDV003	RB010	HDV017	HDV056	HDV071	HDV072	HDV077	HDV081	HDV107	HDV121
Unit	Hidalgo	Hidalgo	Hidalgo	Hidalgo	Hidalgo	Hidalgo	Hidalgo	Hidalgo	Hidalgo	Hidalgo
Lithology	basalt	basaltic andesite	basalt	basaltic andesite	basalt	basalt	basalt	andesite	basalt	andesite
SiO_2	48.68	54.06	49.08	52.35	48.24	47.66	51.79	57.42	48.4	57.6
TiO_2	2.03	1.48	1.42	1.37	1.71	1.99	1.2	0.96	1.71	1.19
Al_2O_3	16.61	17.41	19.35	19.18	17.52	18.34	19.1	18.39	17.79	17.9
FeO	14.25	9.18	9.7	9.08	10.37	11.77	9.37	8.2	9.63	8.31
MnO	0.06	0.14	0.08	0.14	0.13	0.06	0.17	0.11	0.11	0.09
MgO	4.33	2.65	4.94	3.14	4.71	4.51	2.73	2.67	7.02	1.62
CaO	5.75	4.42	7.26	8.13	7.52	4.06	3.49	1.51	7.38	1.81
Na_2O	3.45	3.27	3.27	4.39	3.81	1.66	6.69	6.06	3.37	5.3
K_2O	3.3	2.71	1.21	1.18	1.03	1.98	1.36	1.2	0.98	3.98
P_2O_5	0.06	0.82	0.24	0.31	0.34	0.6	0.8	0.36	0.32	0.22
LOI	2.24	3.36	4.49	1.95	5.06	8.5	3.41	3.58	3.29	1.9
Total	100.76	99.5	101.04	101.22	100.44	101.13	100.11	100.46	100	99.92
Sr	1188	859	855	1349	862	242	1742	1234	1818	940
Ba	736	1417	501	893	374	153	837	1507	576	1548
Y	15.8	30	17	19	23	33	27	19	21	12
Zr	136	207	103	159	122	198	161	176	122	197
Sc	18.3	18	22	10	27	32	9	10	34	10
V	215	191	277	189	242	315	149	122	281	113

Sample	HDV126	HDV127	HDV015	HDV001	HDV039	HDV119	HDV124	HDV111	HDVPCG
Unit	Hidalgo	Hidalgo	Cumulate	dike	dike	dike	dike	Eocene	Hatchet Gap
Lithology	basaltic andesite	basalt	diorite	basalt	basaltic andesite	basaltic andesite	andesite	rhyolite	granite
SiO_2	53.97	51.25	46.22	47.98	55.21	52.96	58.89	70.4	71.52
TiO_2	1.49	1.46	1.9	1.55	0.72	1.12	1.03	0.24	0.25
Al_2O_3	17.71	16.26	15.87	17.88	17.64	17.94	15.75	14.84	12.61
FeO	11.03	11.3	13.23	10.05	6.83	9	6.91	1.84	3.06
MnO	0.14	0.16	0.16	0.06	0.08	0.1	0.06	0.06	0.05
MgO	2.74	3.69	6.45	6.42	2.95	3.85	5.44	0.71	0.03
CaO	3.95	7.25	6.42	6.93	5.16	4.38	0.79	1.45	0.53
Na_2O	5.02	3.83	3.73	2.97	3.75	4.28	6.02	4.34	3.38
K_2O	1.55	1.43	1.05	1.49	3.26	2.4	1.57	3.08	7.48
P_2O_5	0.31	0.15	0.6	0.42	0.35	0.3	0.11	0	0.13
LOI	2.3	1.75	3.43	4.99	5.05	2.55	3.67	1.17	0.86
Total	100.21	98.53	99.06	100.74	101	98.88	100.24	98.13	99.9
Sr	1404	1212	1216	1080	1292	1167	903	723	15
Ba	908	811	431	542	1098	1102	706	1514	70
Y	13	13	26	19	19	23	15	9	172
Zr	159	132	84	105	185	184	146	133	583r
Sc	13	17	28	29	10	17	15	1	1
V	132	166	289	244	118	187	144	17	7

heterolithologic breccias in the Hidalgo Formation suggests that the breccias were also formed during debris flows. The biotite-bearing breccia is interpreted to be the product of an explosive sector collapse or dome collapse, resulting in the incorporation of large clasts of the volcanic structure into a pyroclastic or debris flow.

The basal sedimentary heterolithologic breccia with both igneous and sedimentary clasts is unique to the Ringbone-Hidalgo contact. Well-rounded to sub-rounded sedimentary and small, sub-rounded igneous clasts indicate weathering and transport of igneous clasts prior to deposition or recycling of the sedimentary clasts. Due to the lack of apparent juvenile volcanic clasts and the well-rounded nature of the sedimentary clasts, we interpret this breccia as a debris flow that incorporated alloclastic sedimentary material from a stream bed or slope. This may indicate that a sedimentary clast source from a topographic high shed debris into the basin only early in the volcano's evolution.

Sedimentary rocks

Reworking of adjacent breccia and sedimentary units probably produced conglomerates in the Hidalgo Formation. Abundant volcanic clasts with large hornblende phenocrysts and individual hornblende grains were derived from the underlying sedimentary-volcanic heterolithologic breccia and/or an underlying planar-bedded hornblende-bearing sandstone. The two examples of limestone-clast conglomerate, like the basal heterolithologic breccia, suggests that debris was shed from a source region that contained cobble–boulder-sized clasts of limestone. The topographic relief may have been associated with the Hidalgo uplift or with development of one of the contemporaneous thrusts, which exposed Lower Cretaceous strata to the southwest (Seager and Mack, 1986; Hodgson, 1991; Lawton et al., 1993).

Volcanological model

Hackett and Houghton (1989) presented a volcanological lithofacies association model based on the volcanic and volcaniclastic deposits identified at Ruapehu Volcano, a New Zealand Quaternary volcanic center (Table 3). This volcanological model relies on lithofacies associations to determine the location of a sequence of volcanic deposits relative to the volcanic center. We have modified these models somewhat for comparison with the Hidalgo formation based on studies of breccia deposits at Summer Coon volcano, Colorado, Broken Top volcano, Oregon Cascades, and Ruapehu (Smith and Grubensky, 1993; Grubensky et al., 1998; Smith et al., 1999). Modification of the older models has only affected interpretation of processes of breccia formation and not the location of the deposits relative to the source.

The autobreccias, lava flows, lava flow cores, and debris flows recorded in the Hidalgo Formation represent the proximal cone-forming association of a Laramide volcanic center. This association is dominated by autobrecciated to massive lava flows and heterolithologic breccias. Due to the poor potential for deposition and preservation on the

TABLE 3. Lithofacies associations observed in composite volcanoes.

ASSOCIATION	PRINCIPAL LITHOFACIES	MINOR LITHOFACIES	OTHER FEATURES
Central and flank vent	Irregular lava domes and plug-like intrusions, welded fall deposits, vent breccias	Thin lava flows, lahar deposits	Tectonically oversteepened dips; alteration
Proximal (cone-forming)	Massive and autobrecciated lava flows, lahar deposits	Fall tephra—reworked sediments, dikes, block and ash-flow deposits	Complex gully-filling morphology, numerous apparent stratigraphic inversions
Distal ring plain	Hyper-concentrated and normal stream deposits, fall deposits	Debris avalanche deposits, lava flows, loess	Fall deposits strongly wind influenced
Satellite vent	Strombolian bomb beds, phreatomagmatic surge and fall deposits, aa lava flow	Reworked sediments, distal fall deposits from composite volcano	Relatively primitive chemical composition

steep flanks of a volcano, sedimentary units, pyroclastic block and ash flows, ash- and lapilli-fall deposits, and debris flows are subordinate to the autobrecciated and massive lava flows (Cole et al., 1986; Hackett and Houghton, 1989; Smith and Grubensky, 1993; Smith et al., 1999).

The lithofacies of the upper member of the Ringbone Formation represent the distal ring plain associated with the Hidalgo volcano. Lava flows, accretionary lapilli tuffs, ash fall tuffs, and debris-flow deposits of the upper member of the Ringbone are typical of lithofacies of the distal ring-plain association where preservation of these deposits is most likely (Table 3). The gradational contact between the Ringbone and Hidalgo formations suggests that volcanic deposits in the upper Ringbone record initial Hidalgo volcanism. The Ringbone-Hidalgo contact records the transition between the ring-plain and cone-forming lithofacies that occurred as the expanding cone came to dominate deposition.

GEOCHEMISTRY

Nineteen samples were collected for whole-rock analysis (Table 2). The samples represent lava flows, intrusions, a hornblende-plagioclase cumulate xenolith, and a sample from the Precambrian(?) pluton exposed in the southern Little Hatchet Mountains. Sample preparation, analytical details, and error analysis are discussed in Young (1996). Whole-rock analyses used inductively coupled plasma-atomic emission spectroscopy (ICP). Analytical precision is less than 2% for all the major elements except P_2O_5 (>5%). For the trace elements Sr and Ba, precision is less than 2%. Precision for V, Sc, Zr, and Y ranges between 2% and 4%. Cr and La have precision of 5–11%. Instrumental neutron activation analyses (INAA) were completed on four lava flow or lava flow core samples (Table 4). Analytical precision for these analyses are <2% except for Zn, Rb, Sr, Ce, Nd, Tb, Yb, Lu, and Ta, which range from 2% to 5%. INAA precision for Cr and Zr is between 6% and 13%. The following discussions of geochemistry, including graphical representations, refer to the analyses normalized to volatile-free concentrations with total iron recalculated as FeO.

Lavas and intrusions of the Hidalgo Formation define a trend from basalt (50.6% SiO_2 and 7.3% MgO) to andesite (59.3% SiO_2 and 1.7% MgO). Al_2O_3 concentrations are high, usually greater than 17% (16.3–20%). Na_2O and K_2O concentrations generally range between 1 and 6%. The Ringbone andesitic lava flow consistently falls within the Hidalgo compositional field (Fig. 3). Volatile contents from loss on ignition (LOI) analysis range from 1.3% in fresh rocks to 8.5% in altered samples; most samples contain between 2% and 4% LOI.

Other samples collected include a possible hornblende-plagioclase cumulate xenolith, the rhyolite plug that intrudes the Hidalgo thrust and Precambrian(?) granite (Table 2). The cumulate xenolith falls at the mafic end of the Hidalgo trend (Fig. 3). The rhyolite plug falls on the silicic extrapolation of the Hidalgo trend. The Precambrian(?) granite is characterized by low Sr (15 ppm), Ba (70 ppm), Sc (1 ppm), and high Y (172 ppm) and high Zr (583 ppm), and lies off the Hidalgo trend for these elements.

Rare-earth-element (REE) analyses (Table 4) for four Hidalgo lavas are plotted in Figure 4. Concentrations of the light rare-earth elements increase four-fold, compared to a two-fold increase in the heavy rare-earth-element concentrations as SiO_2 concentrations increase. Pronounced positive Eu anomalies are also present in the three less-silicic Hidalgo lavas. Although present, the anomaly is only very slight in the most evolved sample (HDV-081). This sample also exhibits a slight depletion of the middle rare-earth elements relative to the light and heavy rare-earth elements.

Chondrite-normalized incompatible trace-element abundances are plotted in Figure 5 for four Hidalgo lavas. In this diagram, element incompatibility with mantle minerals decreases to the right, resulting in curves with overall negative slopes. Elements with low mobility in aqueous solutions, such as Y, Ti, Hf, and Zr, show a narrow range of abundance for the lavas and generally exhibit increasing abundances with increasing SiO_2. In contrast, mobile elements, especially Ba and Rb, and to a lesser extent La and Ce, exhibit a much wider range of concentrations. Normalized Ta abundances are lower than La for three of the four samples.

Alteration

The Hidalgo formation has been altered by hydrothermal alteration and weathering during and shortly after deposition as well as during later Laramide and Basin-and-Range tectonism and intrusion of the Eureka stock. Low- to medium-grade propylitic alteration is pervasive in the study area and is concentrated along faults and fractures and adjacent to intrusions. As a result of the alteration, varying amounts of epidote, chlorite, clays, iron hydroxides, and carbonate are found throughout Hidalgo samples; however, reasonably unaltered samples can be found.

Alteration has undoubtedly changed the composition of the Hidalgo samples. Behavior of elements in hydrothermal systems is variable and is dependent on fluid pH, Eh, f_{O2}, temperature, fluid/rock ratios, primary igneous textures, mineral stability, availability of complexing ions in the fluid, presence of secondary host minerals, and location relative

TABLE 4. Trace element analyses of Hidalgo samples by INAA. All data listed in ppm.

Sample	HDV017	HDV056	HDV071	HDV081
Rb	38.7	24.9	34.5	36.4
Cs	4.08	0.74	3.59	5.21
La	6.2	10.6	12.0	24.1
Ce	12.35	21	21.49	43.22
Nd	8.47	13.47	11.09	17.84
Sm	2.40	3.14	2.79	3.12
Eu	1.24	1.76	1.13	1.08
Tb	0.353	0.507	0.437	0.389
Yb	1.188	1.383	1.568	1.609
Lu	0.180	0.208	0.237	0.262
Hf	2.74	3.97	3.10	4.72
Ta	0.327	0.804	0.449	0.848
Th	2.30	3.38	2.91	8.18

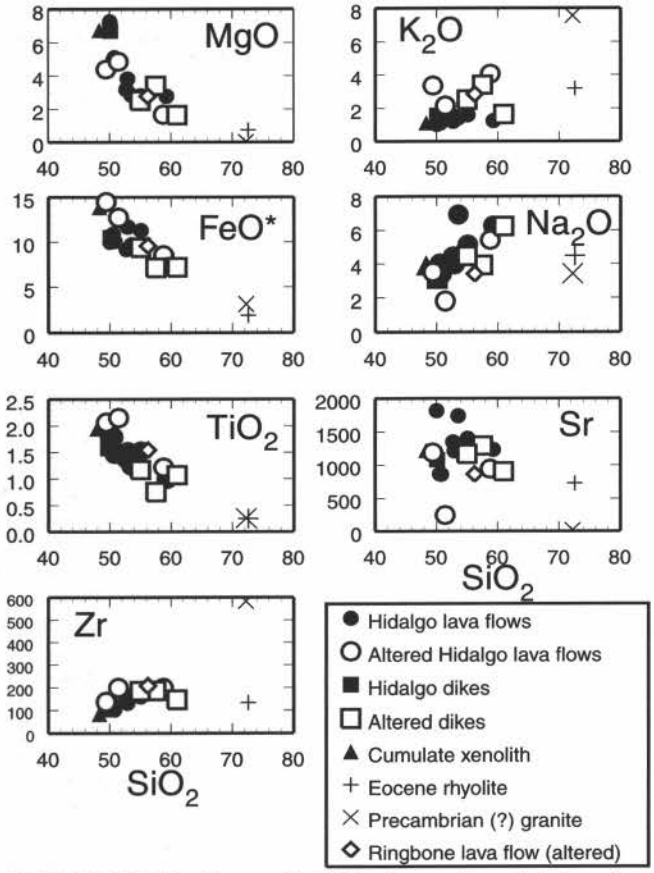

FIGURE 3. Variation diagrams for Hidalgo lavas and associated samples.

to alteration aureole (Badger, 1993; Lecuyer et al., 1994; Fulignate et al., 1999). SiO_2-element plots (Fig. 3) illustrate the extent of alteration in Hidalgo samples. Na_2O and Sr exhibit scatter and poorly correlate with SiO_2. K_2O also exhibits scatter; K_2O concentrations are higher for altered samples than for less-altered samples. Significantly, elements with low solubilities in aqueous solutions (e.g., TiO_2 and Zr) exhibit less scatter and define good magma-evolution trends, suggesting that, although water-rock interaction has changed the concentration of mobile elements, the immobile elements can still be used for chemical classification and petrologic models.

Interpretation

Element mobility in the altered Hidalgo rocks renders conventional magma classification schemes based on the alkalis (Irvine and Baragar, 1971; Le Bas et al., 1985) inapplicable. Thus, we have classified the

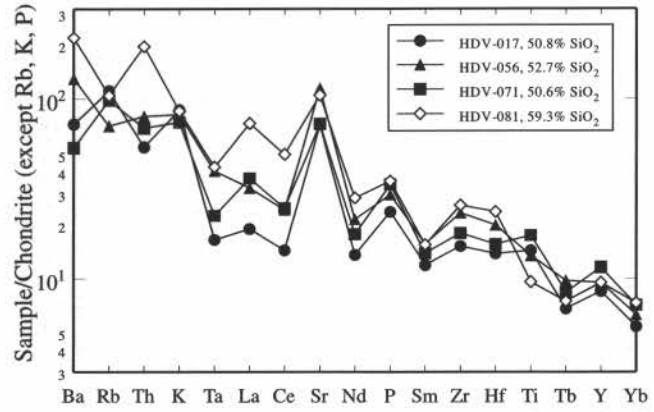

FIGURE 5. Chondrite-normalized incompatible trace element diagrams for four Hidalgo lavas. Normalization values of Thompson (1982) were used.

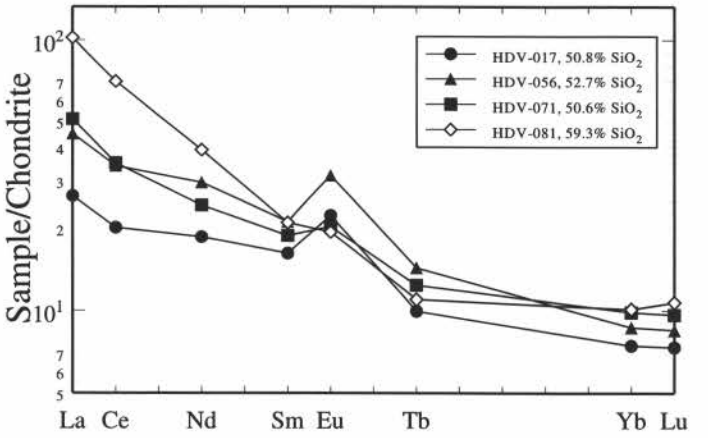

FIGURE 4. Chondrite-normalized rare-earth-element diagrams for four Hidalgo lavas. Chondritic values of Watson (1985) were used.

samples based on their SiO_2 contents (Table 2). Similarly, some compositional schemes that can be used to discern tectonic environment are based at least partly on the alkalis. For instance, the definition of subalkaline vs. alkaline magmas depends on the total alkali concentration (Irvine and Baragar, 1971) and the definition of igneous rocks as peraluminous, peralkaline, or metaluminous is based on the balance between Al_2O_3, CaO, and the alkalis. Thus, our ability to assess the tectonic setting and magma evolution processes of Hidalgo volcanism is hampered by the pervasive alteration of the Hidalgo formation.

Fractional crystallization of hornblende, plagioclase, clinopyroxene, and Fe-Ti oxides was probably the dominant process during evolution of the Hidalgo magmatic system. The phenocryst assemblage differs in mafic and intermediate Hidalgo magmas. Mafic lava flows and dikes typically contain plagioclase, hornblende, and Fe-Ti oxides with or without augite. As differentiation increases (>53% SiO_2), the abundance of hornblende diminishes. The presence of cumulate hornblende-plagioclase-augite cumulate plutonic xenoliths in dikes and lava flows throughout the Ringbone and Hidalgo formations suggests that these minerals were fractionating in the Hidalgo magma chamber. These mineralogic observations are reflected in the geochemistry of Hidalgo samples. An inflection observed (~53% SiO_2) in the MgO-SiO_2 diagram (Fig. 3) is consistent with initial fractionation of hornblende and plagioclase, followed by fractionation of plagioclase with less hornblende. In addition, the rare earth element diagram (Fig. 4) indicates a depletion of the middle rare earth elements in the most evolved magma relative to the more mafic magmas. This pattern is consistent with fractionation of hornblende because hornblende preferentially incorporates the middle rare earth elements relative to the light or heavy rare-earth elements.

Although fractionation of hornblende, plagioclase, and clinopyroxene was the dominant process in the Hidalgo magmatic system, fractional crystallization models underestimate light rare-earth element concentrations, although the middle and heavy rare-earth-element concentrations are easily reconciled with 30% crystallization (Young, 1996), suggesting that assimilation was also an active process. The presence of hornblende with partial to complete reaction coronas of oxides and/or pyroxene implies that crystallization occurred at high P_{H2O} at mid-crustal depths prior to storage in a shallow subvolcanic chamber. Temperatures of crustal rocks at mid-crustal depths would favor assimilation of the wall rock. Diffuse, eroded, and rounded edges of plagioclase, hornblende and quartz xenocrysts also suggest that assimilation was an active process. Quartz xenocrysts suggest a high-silica contaminant; however, high concentrations of Zr (583 ppm) and Y (172 ppm), and the low concentration of Ba (70 ppm) in the Precambrian(?) Hatchet Gap granite preclude models that use it as a contaminant (Fig. 3).

The Hidalgo volcano exhibits several characteristics of continental arc volcanoes. These include lack of primitive compositions, dominantly andesitic lavas, crystallization of plagioclase-hornblende ± augite, and a variety of eruptive styles resulting in a composite cone. The incompati-

ble trace-element compositions of the lavas support the idea that the Hidalgo Formation represents subduction-related magmatism. Arc magmas are typically depleted in the high-field-strength elements Ta, Nb, Ti, and Zr relative to the soluble elements Ba, Rb, K, and Sr. Unfortunately, extensive alteration and mobility of the soluble elements renders these elements unsuitable for discriminating between tectonic settings. However, Ta has lower chondrite-normalized abundances than La for most of the Hidalgo lavas analyzed (Fig. 5), consistent with an arc origin for Hidalgo volcanism.

CONCLUSIONS

The Hidalgo Formation is composed predominantly of autobrecciated lava flows, debris flows and lava flows with subordinate sedimentary deposits, dikes and plugs. Based on the lithofacies assemblage, the Hidalgo represents the proximal cone-forming facies of a Laramide composite cone (Lawton et al., 1993; Young, 1996). $^{40}Ar/^{39}Ar$ age determinations of 70.53 ± 0.48, 70.69 ± 0.44 Ma, and 71.49 ± 0.38 Ma firmly establish the age of the Hidalgo Formation as Late Cretaceous. Subplinian and strombolian eruptions as well as magmatic extrusions from domes and lava flows similar to the eruptions documented at Ruapehu, a modern composite cone (Cole et al., 1986; Hackett and Houghton, 1989) all contributed to growth of the cone. The age of the Hidalgo Formation provides an age constraint for deformation late in the Laramide orogeny, in which the Hidalgo cone was folded into an overturned-footwall syncline adjacent to the Hidalgo thrust fault (Zeller, 1970; Hodgson, 1991; Lawton et al., 1993; Young, 1996).

Initiation of Hidalgo volcanism occurred during deposition of the upper Ringbone Formation. Upper Ringbone deposits represent the distal ring plain of the Hidalgo volcanic center, as indicated by the intercalation of tuffaceous sandstones, volcanic breccia deposits, accretionary lapilli deposits and lava flows with normal Ringbone fluvial deposits. The upper Ringbone–Hidalgo Formation contact represents the transition from ring plain to proximal cone-forming lithofacies deposition resulting from increased influence of an expanding breccia-dominated Laramide volcanic center onto the surrounding ring plain.

Lavas and intrusions of the Hidalgo Formation range from basalt to rhyolite but are dominated by andesite. Petrographic and geochemical data indicate fractional crystallization of hornblende, plagioclase, and clinopyroxene, coupled with assimilation, controlled the evolution of the Hidalgo magmatic system. High concentrations of Zr and Y of the Precambrian(?) Hatchet Gap granite preclude it as an assimilant. Hidalgo incompatible trace-element patterns are consistent with modern continental volcanic arcs and suggest that low-angle subduction of the Farallon plate beneath the western margin of North America triggered magma generation.

ACKNOWLEDGEMENTS

Partially supported by the Clemons Field Scholarship (NMSU). Matt Heizler and David Broxton reviewed an earlier version of this paper; their suggestions greatly improved the manuscript.

REFERENCES

Badger, R. L., 1993, Fluid interaction and geochemical mobility in metabasalts: An example from the central Appalachians: Journal of Geology, v. 101, p. 85–95.

Basabilvazo, G. T., 1991, Stratigraphy, depositional environments, and sediment dispersal pathways of the Upper Cretaceous Ringbone Formation in the Little Hatchet Mountains of southwestern New Mexico [M.S. thesis]: Las Cruces, New Mexico State University, 158 p.

Cole, J. W., Graham, I. J., Hackett, W. R. and Houghton, B. F., 1986, Volcanology and petrology of volcanoes of the Tongariro Volcanic Centre, Taupo Volcanic Zone: Royal Society of New Zealand Bulletin, v. 23, p. 224–250.

Coney, P. J. and Reynolds, S. J., 1977, Cordilleran Benioff zones: Nature, v. 270, p. 641–644.

Dickinson, W. R. and Snyder, W. S., 1978, Plate tectonics of the Laramide orogeny: Geological Society of America, Memoir 151, p. 355–366.

Dickinson, W. R., Snyder, W. S. and Silberman, M. L., 1976, Tectonic implication of space-time patterns of Cenozoic magmatism in the western United States: Earth and Planetary Science Letters, v. 32, p. 91–106.

Grubensky, M. J., Smith, G. A. and Geissman, J. W., 1998, Field and paleomagnetic characterization of lithic and scoriaceous breccias at Pleistocene Broken Top volcano, Oregon Cascades: Journal of Volcanology and Geothermal Research, v. 83, p. 93–114.

Fulignate, P., Gioncada, A. and Sbrana, A., 1999, Rare-earth element (REE) behaviour in the alteration facies of the active magmatic-hydrothermal system of Vulcano (Aeolian Islands, Italy): Journal of Volcanology and Geothermal Research, v. 88, p. 325–342.

Hackett, W. R. and Houghton, B. F., 1989, A facies model for a Quaternary andesitic composite volcano: Ruapehu, New Zealand: Bulletin of Volcanology, v. 51, p. 51–68.

Hodgson, S. A., 1991, Geology and tectonics of the northern Little Hatchet Mountains, Grant and Hidalgo counties, southwestern New Mexico [M.S. thesis]: Las Cruces, New Mexico State University, 117 p.

Irvine, T. N. and Baragar, W. R. A., 1971, A guide to the chemical classification of the common volcanic rocks: Canadian Journal of Earth Sciences, v. 8, p. 523–548.

Kay, S. M. and Abbruzzi, J. M., 1996, Magmatic evidence for Neogene lithospheric evolution of the Central Andean "flat-slab" between 30ºS and 32ºS: Tectonophysics, v. 259, p. 15–28.

Keith, S. B. and Wilt, J. C., 1986, Laramide orogeny in Arizona an adjacent regions—A strato-tectonic synthesis; *in* Beatty, B., and Wilkinson, P. A. K., eds., Arizona Geological Society Digest, v. 16, p. 502–554.

Lawton, T. F., Basabilvazo, G. T., Hodgson, S. A., Wilson, D. A., Mack, G. H., McIntosh, W. C., Lucas, S. G. and Kietzkie, K. K., 1993, Laramide stratigraphy of the Little Hatchet Mountains, southwestern New Mexico: New Mexico Geology, v. 15, p. 9–15.

Lecuyer, C., Gruau, G., Anhaeusser, C. R. and Fourcade. S., 1994, The origin of fluids and the effects of metamorphism on the primary chemical compositions of Barberton komatiites—New evidence from geochemical (REE) and isotopic (Nd, O, H, $^{39}Ar/^{40}Ar$) data: Geochimica et Cosmochimica Acta, v. 58, p. 969–984.

Le Bas, M. J., LeMaitre, R. W., Streckeisen, A. and Zanettinm, B., 1986, A chemical classification of volcanic rocks based on the total alkali-silica diagram: Journal of Petrology, v. 27, part 3, p. 745–750.

Lipman, P. W. and Sawyer, D. A., 1985, Mesozoic ash-flow caldera fragments in southeastern Arizona and their relation to porphyry copper deposits: Geology, v. 13, p. 652–656.

Loring A. K. and Loring, R. B., 1980, Age of thrust faulting, Little Hatchet Mountains, southwestern New Mexico: Isochron/West, v. 27, p. 29–30.

Parsons, W. H., 1969, Criteria for the recognition of volcanic breccias: review: Geological Society of America, Memoir 115, p. 263–304.

Seager, W. R. and Mack G. H., 1986, Laramide paleotectonics of southern New Mexico: American Association of Petroleum Geologists, Memoir 41, p. 669–685.

Smith, G. A., 1986, Coarse-grained non-marine volcaniclastic sediment: Terminology and depositional process: Geological Society of America Bulletin, v. 97, p. 1–10.

Smith, G. A. and Grubensky, M. J., 1993, Toward a facies model for breccia-dominated composite volcanoes: The Oligocene Summer Coon volcano, Colorado (abs.), EOS, v. 74, p. 644.

Smith, G. A., Grubensky, M. J. and Geissman, J. W., 1999, Nature and origin of cone-forming volcanic breccias in the Te Herenga Formation, Ruapehu, New Zealand: Bulletin of Volcanology v. 61, p. 64–82.

Snyder, W. S., Dickinson, W. R. and Silberman, M. L., 1976, Tectonic implications of space-time patterns of Cenozoic magmatism in the western United States: Earth and Planetary Science Letters, v. 32, p. 91–106.

Thompson, R. N., 1982, Magmatism of the British Tertiary Volcanic Province: Scottish Journal of Geology, v. 18, p. 49–107.

Titley, S. R. and Anthony, E. Y., 1988, Laramide mineral deposits in Arizona; *in* Jenney, J. P. and Reynolds, S. J., eds., Geological Evolution of Arizona: Arizona Geological Digest, v. 17, p. 485–514.

Watson, J. T., 1985, Meteorites: their record of early solar-system history: W. H. Freeman, USA, 267 p.

Young, J. R., 1996, Volcanology and geochemistry of the Upper Cretaceous–Lower Tertiary Hidalgo Formation: Remnant of a Laramide volcanic center, southwestern New Mexico [M.S. thesis]: Las Cruces, New Mexico State University, 95 p.

Zeller, R. A., 1970, Geology of the Little Hatchet Mountains, Grant and Hidalgo counties: New Mexico Bureau of Mines and Mineral Resources, Bulletin 96, 22 p.